J. Electrochem. Sci. Eng. **16** (2026) 3330; https://doi.org/10.5599/jese.3330

Open Access : : ISSN 1847-9286
https://pub.iapchem.org/ojs/index.php/JESE

Original scientific paper

Electrochemical properties of nickel manganese cobalt oxide cathode material obtained during battery recycling

Hanna Potapenko[1,2], Oleksandr Potapenko[1,2,3], Vitalii Sirosh[1], Zhou Chang Ji[2,5], Zhou Hui[2], Borys Haliuk[4], Chee Sien Wong[2,3] and Viacheslav Barsukov[4,✉]

[1]*V.I. Vernadsky Institute of General and Inorganic Chemistry of the NAS of Ukraine, Acad. Palladina Ave 32/34, Kyiv, 03142, Ukraine*
[2]*Zhejiang Casnovo New Materials Co., Ltd., No.1 Zhongke Road, Zhanmao Street, Putuo District, Zhoushan City, Zhejiang Province, China*
[3]*School of Petrochemical Engineering and Environment, Zhejiang Ocean University, No. 1, Haida South Road, Lincheng Street, Dinghai District, Zhoushan City, Zhejiang Province, China*
[4]*Institute for Sorption and Problems of Endoecology of the National Academy of Science of Ukraine, 13, Olega Mudraka str., Kyiv 03164 Ukraine*
[5]*Institute of Materials Research and Engineering, Singapore*

Corresponding Author: ✉*v-barsukov@i.ua*

Received: April 12, 2026; Accepted: September 16, 2026; Published: November 12, 2026

Abstract

Recycling spent batteries, particularly lithium-ion batteries, is becoming a global priority. Among the various recycling approaches, hydrometallurgy is one of the most useful methods. Among the many chemical compositions of cathode materials, ternary layered oxides warrant particular attention in recycling technology, making them more suitable candidates than other cathode materials. During hydrometallurgical leaching, various carboxylic acids are employed as solvents; however, oxalic acid deserves special consideration due to its high selectivity for lithium extraction. Nickel, cobalt, and manganese oxalates are practically insoluble in water and exist as the corresponding crystal hydrates. When a solution of transition metal sulphates, derived from cathode powder, is treated with a mixture of oxalic acid, the lithium remains in solution as a mixture of lithium sulphate and oxalate, while the transition metals are converted into their corresponding oxalates. In this process, a significant increase in the mass of the precipitate is observed, corresponding to the formation of oxalates. Thus, oxalic acid enables selective extraction of lithium from the "black mass" of lithium-ion batteries based on layered transition metal oxides. Moreover, the resulting mixture of transition metal oxalates, after minor compositional adjustments, can be directly reused for the resynthesis of ternary layered oxides. This paper presents methods for the hydrometallurgical processing of NCM523 (lithium nickel-cobalt-manganese oxide with a 5:2:3 molar ratio of Ni:Co:Mn) cathode material and its subsequent re-synthesis using transition metal and lithium oxalates. The physicochemical charac-

teristics and electrochemical properties of the regenerated NCM523 electrodes are evaluated from the perspective of their potential reuse in rechargeable power sources.

Keywords
Spent batteries, battery cathode recovery, ternary layered oxides, oxalic acid leaching, electrochemical tests

Introduction

Among the wide range of chemical compositions available for cathode materials, ternary layered oxides (NCM - $LiNi_xCo_yMn_zO_2$) warrant particular attention in recycling technology, making them more suitable candidates for recycling compared to other cathode materials, such as $LiFePO_4$ (LFP) [1-3]. This priority is justified by several key factors:

(i) High cost and critical raw materials: NCM cathodes contain significant amounts of cobalt and nickel metals characterized by high cost, limited geological reserves, and geopolitical supply risks. Recovering these metals from spent batteries is economically more profitable than primary extraction from ores, as confirmed by calculations of the elemental composition of different LIB types (see Table 1) [4].

Table 1. *Mean values for individual cells [4]*

	Cell type		
	NCM	NCA	LFP
Total battery mass, kg	141	100	118
Total mass of battery (normalized), g	1000	1000	1000
Energy recovered from recycling batteries, kWh / T	86	96	71
Cell materials			
	Content, g kg^{-1}		
Total	630	598	530
Cathode	191	175	173
Lithium	14	13	7.6
Cobalt	39	16	0
Nickel	39	86	0
Manganese	36	0	0
Aluminum	0	2.5	0
Iron	0	0	61
Phosphorus	0	0	34
Oxygen	63	58	70
Electrolyte	114	101	85
Separator	54	50	43
Anode-carbon	140	131	111
Cathode foil - Al	39	40	34
Anode foil - Cu	66	70	60
Cell case - Al	21	20	17
Others	6	10	8.5
Battery and cell housing			
Total	370	402	470
Cables	21	50	64
Copper	13	30	38
Aluminum	1.4	10	13
Stainless steel	7.1	10	13
Frame	114	101	128
Plastics	107	81	102
Stainless steel	7.1	20	26
Casing (stainless steel)	199	241	267
Others	36	10	11

(cc) BY

(ii) Energy density and application scope: NCM-based batteries dominate the high-performance electric vehicle market, where high energy density is essential. Consequently, most end-of-life electric vehicles in the coming years will contain NCM-based batteries, generating substantial and relatively uniform waste streams ideal for large-scale recycling operations.

(iii) Ecological footprint: The production of NCM cathodes, particularly nickel-rich compositions, carries a significant energy and carbon footprint due to energy-intensive processing. Recycling can substantially mitigate this environmental burden compared to primary production.

Because battery sizes and chemical compositions vary widely, calculating the relative mass of their constituent materials is not straightforward. To address this issue, a battery mass model incorporating various cell chemistries was developed in [4]. This model is based on research into the average weight and material composition of the three most prevalent battery types: lithium nickel cobalt manganese oxide (NCM), lithium nickel cobalt aluminum oxide (NCA), and lithium iron phosphate (LFP). The consolidated results of this analysis are presented below in Table 1.

Although a variety of techniques for processing electrode materials have been reported [5-8], hydrometallurgy is the predominant method employed on an industrial scale. The choice of a leaching reagent for metal recovery is dictated by the need to balance extraction efficiency, cost-effectiveness, and adherence to environmental regulations.

Hydrometallurgical processing of NCM cathodes is based on the principle of completely dissolving valuable metals, followed by their selective extraction from the solution. The process typically consists of three main stages: (i) mechanical and chemical pretreatment (discharging and dismantling the battery casing, separating components and obtaining the "black mass"), (ii) leaching (transferring metal oxides into a soluble form), and (iii) separation and purification (isolating individual metals or their compounds). The key link is the leaching stage, where the choice of reagent determines the efficiency, cost-effectiveness, and environmental friendliness of the entire process. A mixture of H_2SO_4 and H_2O_2 is the best option for large-scale leaching (or dissolution) of NCM cathodes [9,10] due to the cheapness and high degree of dissolution of the components of "black mass".

Among the carboxylic acids evaluated, oxalic acid ($H_2C_2O_4$) has garnered particular attention due to its high efficiency and selectivity for lithium extraction [9]. The process capitalizes on the low aqueous solubility of the resultant nickel, cobalt, and manganese oxalates, which precipitate as crystalline dehydrates ($Me_2C_2O_4 \cdot H_2O$). However, the degree of black mass dissolution in $H_2C_2O_4$ and 10 % H_2O_2 is lower than in the H_2SO_4/H_2O_2 system. Therefore, it is necessary to treat the black mass not directly with oxalic acid, but with H_2SO_4/H_2O_2. Upon mixing these solutions, the transition-metal sulfates convert to insoluble oxalates, while lithium remains in solution as a mixture of sulfates and oxalates.

After minor compositional adjustments, the resulting precipitate of mixed transition-metal oxalates can be used as a precursor for synthesizing layered oxide cathode materials [11,12].

This paper details a hydrometallurgical process for treating $LiNi_{0.5}Co_{0.2}Mn_{0.3}O_2$ (NCM532) cathode material harvested from commercial lithium-ion batteries. The study encompasses both the leaching stage with oxalic acid and the subsequent re-synthesis of the NCM layered oxide from the generated transition metal and lithium oxalates.

Experimental

A cell that had sustained a capacity loss exceeding 40 % of its nominal value was discharged to a cutoff voltage of ~0.5 V using a constant resistive load. The casing was subsequently cut along its contour under controlled conditions to mitigate the risk of short circuits and thermal runaway. Finally, the positive and negative electrodes, along with the separator, were mechanically harvested.

Subsequently, the cathode material composed of layered $LiNi_xCo_yMn_zO_2$, amorphous carbon and a polymer binder was mechanically separated from the aluminum foil. To eliminate the polymer binder, the material was subjected to thermal annealing at ~400 °C for several hours. The resulting black powder served as a precursor for the hydrometallurgical process.

Next, the layered oxide was leached in a 5 M H_2SO_4 solution containing ~10 wt.% H_2O_2 at a 1:10 solid-to-liquid ratio. The mixture was stirred vigorously for 24 hours at room temperature, resulting in complete dissolution of the material, except for trace carbon residues (<1 wt.%) that were not eliminated prior to annealing.

The reaction converted the cathode material entirely into soluble sulfates, which were then separated from the insoluble carbon by filtration. Following inductively coupled plasma optical emission spectroscopy (ICP-OES) analysis (ICP spectrometer iCAP 6500 DUO Thermo Electron Corp.) (Table 2), the sulfate solution's composition can be adjusted, if required, to meet the desired Ni:Co:Mn ratio of 5:2:3.

Table 2. *Results of ICP-OES analysis after NCM523 cathode leaching*

Element	Wavelength, nm	Concentration of elements in 5 M H_2SO_4 + 10 % H_2O_2 solution, g L^{-1}
Al	396.1	< 0.05
Cu	324.7	< 0.05
Ni	231.6	7.36
Li	670.7	1.59
Co	230.7	2.88
Mn	279.4	4.43

The elemental concentrations were measured with an error margin of less than 3 %. As shown in Table 2, the transition-metal ratio (Ni:Co:Mn) matches the target stoichiometry of 5:2:3, so compositional correction was unnecessary. However, lithium concentration was found to be ~91.4 % of its nominal value. According to our previous findings [13], this lithium deficiency during LIB degradation is attributed to the formation of electrochemically inactive compounds on the anode surface, specifically the solid-electrolyte interphase (SEI) film. Once these compounds form, the lithium concentration in the cathode material cannot be restored, even after deep discharge. Therefore, lithium correction, accounting for a 5 % excess, is performed during the precursor preparation stage, prior to thermal annealing. Notably, no foreign elements such as aluminum or copper, which could potentially leach into the solution during hydrometallurgical processing, were detected.

The reaction between the resulting metal sulfates and excess oxalic acid in an aqueous medium is presented by Equations (1) to (4):

$$Li_2SO_4 + H_2C_2O_4 \rightarrow Li_2C_2O_4 + H_2SO_4 \quad (1)$$

$$CoSO_4 + H_2C_2O_4 \rightarrow CoC_2O_4\downarrow + H_2SO_4 \quad (2)$$

$$NiSO_4 + H_2C_2O_4 \rightarrow NiC_2O_4\downarrow + H_2SO_4 \quad (3)$$

$$MnSO_4 + H_2C_2O_4 \rightarrow MnC_2O_4\downarrow + H_2SO_4 \quad (4)$$

The resulting transition-metal oxalates were then repeatedly washed with distilled water to remove acid residues. Washing continued until the rinse water pH reached approximately 7. The purified oxalates were then dried at ~50° C in a drying cabinet to obtain the $MeC_2O_4{\cdot}2H_2O$ crystalline hydrates. The phase composition of the obtained crystal hydrates was confirmed by DTA analysis (BonninTech, STA200, Wuhan, China). All transition-metal oxalate samples were heated at a rate of 10 °C min^{-1}. After separation of the transition metal oxalates, the remaining lithium oxalate solution (acidified with sulfuric acid) was treated with alkali to precipitate lithium carbonate in accordance with the following procedure [14,15].

(cc) BY

The obtained transition metal hydrate crystals, with a Ni:Co:Mn ratio of 5:2:3, were introduced into a Li oxalate ($Li_2C_2O_4$) solution prepared from oxalic acid and lithium carbonate. The lithium-to-transition metal mixture ratio was maintained at 1.05:1, with this 5 % lithium excess intended to compensate for lithium losses typically observed at elevated synthesis temperatures [16-18]. To minimize particle agglomeration during synthesis, glucose was added to the lithium oxalate solution at 20 % of the total reagents' mass.

For homogenization and particle size reduction, the solution containing the transition-metal oxalates was subjected to ultrasonic treatment for 1 hour at ~500 W. The resulting mixture was then placed in a drying cabinet at 100 °C until complete solvent evaporation. The obtained powder served as the precursor for NCM523 synthesis.

The formation of single-phase $LiNi_{0.5}Co_{0.2}Mn_{0.3}O_2$ was achieved through thermal treatment at 890 °C for 12 hours in an air atmosphere according to Equation (5):

$$0.5\ Li_2O + 0.5\ NiO + 0.067\ Co_3O_4 + 0.15\ Mn_2O_3 + 0.142\ O_2 \rightarrow LiNi_{0.5}Co_{0.2}Mn_{0.3}O_2 \quad (5)$$

The heating and cooling rates within the muffle furnace were maintained at 4.5±0.5 °C min^{-1}. The final product was a black NCM52 powder, which was subsequently used in further investigations.

Electrochemical tests

The 2025 coin cells were assembled in an argon-filled glove box (Mikrouna (Shanghai) Ind. Int. Tech. Co., Ltd., China) with controlled H_2O and O_2 concentrations below 5 ppm. A 1 M solution of lithium hexafluorophosphate ($LiPF_6$) in ethylene carbonate/dimethyl carbonate/ethyl methyl carbonate (EC/DMC/EMC, 1:1:1 volume ratio) was used as the electrolyte (Dongguan Shanshan Battery Material Co. Ltd., China). A Celgard 2500 membrane (porosity: 55 %) was used as the separator, and lithium metal served as the auxiliary electrode. The active material mass in the electrode was 20±0.5 mg, and the electrode area was 2 cm^2. The assembled coin cells were rested for 24 hours before electrochemical testing.

The electrochemical performance of the electrodes was evaluated using a CHI electrochemical workstation (CH Instruments Inc., USA) and a Neware battery tester (Neware, China). Galvanostatic charge/discharge cycling was performed at current rates varying from 0.05C to 5C over a potential range of 3.0 to 4.5 V.

Results and discussion

The NCM523 precursor material was derived from a spent lithium-ion battery assembled *via* laminate technology (Figure 1).



Figure 1. *The emergence of the lithium-ion battery featuring an NCM523 cathode*

For accurate identification of the phase-transition temperature of the Ni:Co:Mn (5:2:3) oxalates, DTA was conducted on oxalates obtained from sulfate-based solutions.

The thermal decomposition of transition metal oxalates MeC_2O_4 (where Me = Ni, Co, Mn) is shown in Figure 2. In air, it proceeds *via* two main stages: (i) dehydration involving the removal of water of crystallization, and (ii) decomposition of the resulting anhydrous oxalates into metal oxides.

As shown in the graph, the first sharp mass loss of Mn, Co and Ni oxalates (an endothermic process) occurs at 146, 218 and 260 °C, respectively. The increase in dehydration temperature is primarily related to the crystal lattice energy.

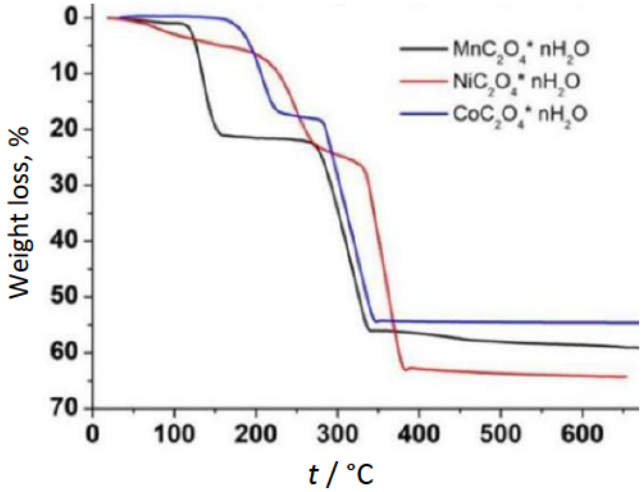


Figure 2. *Mass loss of Mn, Ni, and Co oxalates during thermal heating*

It is known that in the series $Mn^{2+} > Co^{2+} > Ni^{2+}$, the ionic radius decreases (Mn^{2+}: ~0.083 nm; Co^{2+}: ~0.0745 nm; Ni^{2+}: ~0.069 nm). The smaller the ion, the more strongly it attracts water molecules; therefore, the Ni^{2+}-$2OH^-$ bond is the strongest among these three metals. Accordingly, breaking this bond to "push" the water molecule out of the crystal lattice requires more energy, which corresponds to a higher temperature. The mass loss during the dehydration stage was 21.1, 17.4 and 23.0 wt.% for Mn, Co and Ni, respectively, which corresponds to 2.1, 1.8 and 2.5 M of H_2O, respectively. The presence of 0.5 moles of free moisture during the dehydration of nickel oxalate is confirmed by a slow mass loss (~3 %) in the temperature range of 50 to 140 °C. The decomposition of anhydrous oxalate occurs at higher temperatures: 324, 330 and 374 °C for Mn, Co and Ni, respectively.

NCM523 was synthesized by the heat treatment of a mixture of the corresponding oxalates in two stages:

I. Heating and holding at 490 °C for 6 h. At this temperature, oxalates decompose vigorously into a mixture of oxides to form an ash-like powder, Equations (6) to (9):

$$Li_2C_2O_4 + ½O_2 \rightarrow Li_2O + 2CO_2\uparrow \quad (6)$$

$$3CoC_2O_4 + 2O_2 \rightarrow Co_3O_4 + 6CO_2\uparrow \quad (7)$$

$$NiC_2O_4 + ½O_2 \rightarrow NiO + 2CO_2\uparrow \quad (8)$$

$$2MnC_2O_4 + ½O_2 \rightarrow Mn_2O_3 + 4CO_2\uparrow \quad (9)$$

At 490 °C in an oxygen or air atmosphere, cobalt and manganese oxalates, unlike nickel, are oxidized to higher oxides, and lithium oxalate decomposes directly to its oxide without the intermediate stage of carbonate formation, which is characteristic of annealing in a nitrogen atmosphere [19].

II. A single-phase $LiNi_{0.5}Co_{0.2}Mn_{0.3}O_2$ cathode material with an α-$NaFeO_2$ type layered structure was synthesized by annealing at 890 °C for 12 h in air (Equation 5). Prior to annealing, the oxide precursor mixture was thoroughly ground in an agate mortar to ensure homogenization. The

(cc) BY

prolonged high-temperature treatment promoted solid-state ion diffusion, removed residual impurities, and produced a highly crystalline product.

The heating/cooling rate of the sample in the muffle furnace was maintained within the range of 4.5±0.5 °C min^{-1} for both stages of heat treatment.

The phase composition, morphology, and particle size of the obtained compounds were analyzed using X-ray diffraction (XRD) (DX-2700BH, Dandong Haoyuan Instruments, China, CuK_α) and scanning electron microscopy (SEM) (JSM-6700f, JEOL, Japan). XRD measurements were performed at room temperature over a 2θ range from 10 to 80° with a step size of 0.05°. Crystallite sizes were determined using the Scherrer equation for (003) and (104) peak broadening.

In the layered structure of $LiNi_{0.5}Co_{0.2}Mn_{0.3}O_2$, the (003) and (104) reflections provide distinct information (Figure 3). Specifically, the (003) reflection is sensitive to the degree of cation ordering between the Li layer (site 3a) and the transition metal (TM) layer (site 3b).

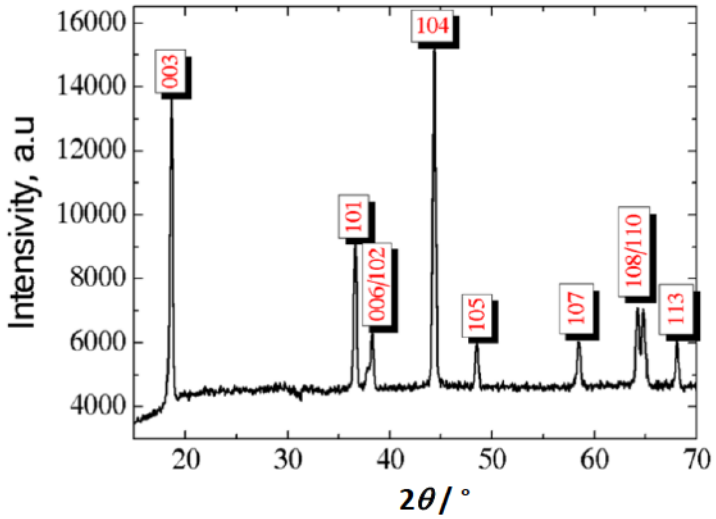


Figure 3. *X-ray diffraction pattern of NCM523*

The intensity of the (003) peak decreases if Ni^{2+} ions migrate into the Li layer, because Ni and Li have different X-ray scattering factors. The intensity of the (104) peak is influenced by the transition metal sublattice. Consequently, a peak ratio ($I_{003/104}$) below 1 indicates significant cation mixing or partial disordering (Table 3) [20-22].

Table 3*. Crystallographic parameters of the structure of NCM523 samples, space group R3m*

	a / nm	*c* / nm	*c* / *a*	$I_{003/104}$	Crystallite size, nm	Ref.
Sample 1	0.28636	1.4211	4.963	1.51	49	[23]
Sample 2	0.28601	1.4233	4.976	1.48	54	
Sample 3	0.28747	1.4259	4.960	0.89	60	This paper

Several factors may contribute to this disordering: (i) insufficient synthesis temperature; incomplete cation diffusion prevents full ordering; (ii) non-stoichiometric oxygen content, where the presence of oxygen vacancies facilitates the migration of Ni^{2+} ions; (iii) deviations in stoichiometry where an excess of nickel or a deficiency in lithium increases the degree of site mixing; (iv) excessively rapid quenching after calcination. This process can capture a disordered structure.

Ultimately, such cation mixing blocks Li^+ diffusion pathways, resulting in slower lithium-ion transport. This leads to a lower initial discharge capacity and a reduced charge rate for the material.

In contrast to the synthesized sample, the NCM materials obtained by the method described in [23] exhibited I_{003}/I_{104} peak intensity ratio exceeding 1.2, with values of 1.48 and 1.51. This indicates

minimal cationic mixing and is consistent with previous conclusions. It is worth noting that all samples retained *c/a* values above 4.899, confirming a well-developed hexagonal α-$NaFeO_2$-type structure.

The morphology of the synthesized sample is shown in Figure 4. As can be observed, under these synthesis conditions, the crystallites form aggregates ranging in size from 1 to 2 µm.

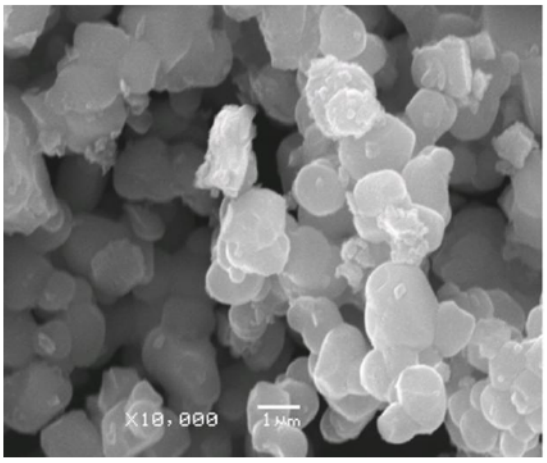


***Figure 4**. SEM image of NCM 523*

The structural characteristics of the samples in Table 2 agree well with their electrochemical performance. As shown in Figure 5, the NCM523 electrode exhibited an initial specific capacity of 131 mAh g^{-1} at 0.1 C, which progressively increased to 144 mAh g^{-1} with further cycling. However, the initial capacities reported by other groups are typically in a higher range, reaching ~180 mAh g^{-1} at low currents in the first few cycles [24-28].

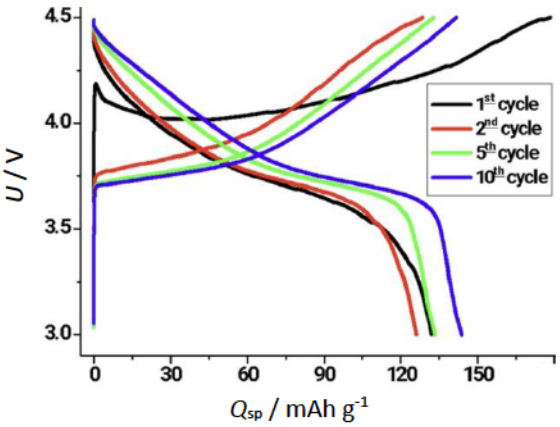


***Figure 5.** Charge-discharge curves, voltage (U) vs. specific capacity (Q_{sp}), of the synthesized NCM523 (cycles 1 to 10). Voltage range: 3.0 to 4.5 V; current rate: 0.1C; temperature: 25 °C*

When switching to higher current densities, the specific capacity of the material decreases as expected (Figure 6 (a)). However, during electrochemical testing, our synthesized NCM523 sample demonstrates the ability to withstand high current loads. For instance, at 3C charge/discharge, the specific capacity of the electrodes is almost half the initial value, specifically 57 mAh g^{-1}, and at 5C, it drops to approximately 20 mAh g^{-1}. Upon reducing the current rate back to 0.05C, the specific capacity is restored to 165 mAh g^{-1}. This value not only exceeds the material's initial specific capacity but is also comparable to that of commercial analogues.

The long-term cycling of NCM523 at various current rates is presented in Figure 6(b). At the beginning of the test, both the specific capacity (Q_{sp}) and coulombic efficiency increased. This initial rise is primarily attributed to the gradual activation of cathode material, likely due to significant particle aggregation. From the 10th cycle onward, the specific capacity stabilizes, and the coulombic

(cc) BY

efficiency remains consistently high at 99.5±0.2 %. Notably, the specific capacity around cycles 90 to 95 at 0.05C exceeds the material's initial specific capacity. This behavior indicates excellent structural stability and resilience during prolonged cycling.

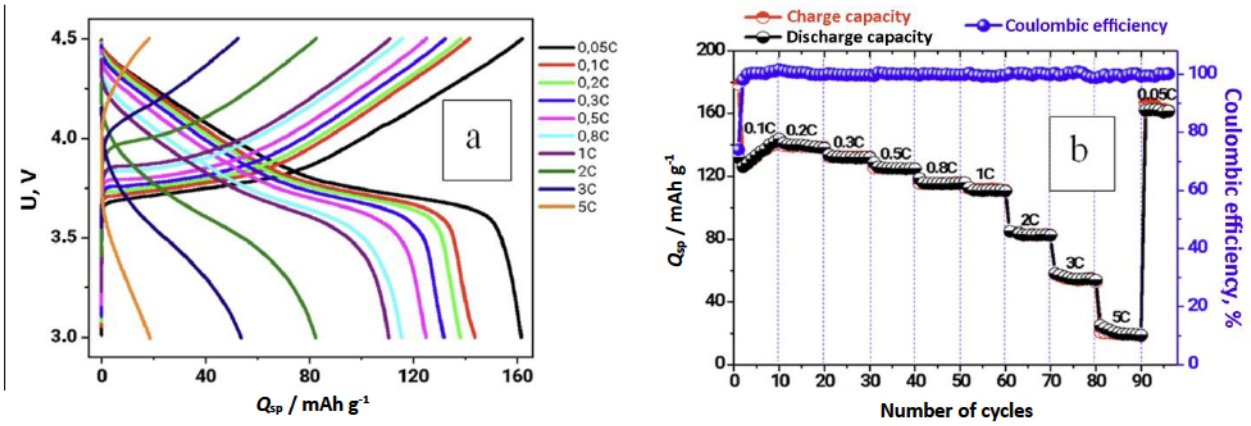


Figure 6. *(a) Charge-discharge curves of NMC523 cathodes in the potential range of 3.0 to 4.5 V at various C - rates and 25° C; (b) galvanostatic cycling performance and coulombic efficiency of NCM523 cathode material at different C - rates (25° C)*

Conclusions

The article proposes a hydrometallurgical method for processing spent NCM532 cathode material, based on the selective precipitation of transition metal oxalates using oxalic acid. This approach keeps lithium in solution, which, after minor adjustment, can be used for subsequent re-synthesis of the material. The resulting mixture of transition metal oxalates (Ni:Co:Mn = 5:2:3) was successfully used as a precursor for the re-synthesis of $LiNi_{0.5}Co_{0.2}Mn_{0.3}O_2$ (NCM523) *via* a two-step solid-state reaction. XRD confirmed that the regenerated material has a hexagonal α-$NaFeO_2$ layered structure; however, the intensity ratio I_{003}/I_{104} = 0.89 indicates significant cation mixing, reflected in the lower specific capacity of the sample. Electrochemical tests revealed an initial specific capacity of 131 mAh g^{-1} at 0.1C, which gradually increased to 144 mAh g^{-1} during cycling. The material demonstrates good rate capability: at 3C, the capacity is ~57 20 mAh g^{-1}, and after returning to 0.05C, the specific capacity recovers to 165 mAh g^{-1}, comparable to commercial NCM523. The coulombic efficiency during cycling is 99.5±0.2 %.

Therefore, to further enhance the electrochemical performance of NCM electrodes in the subsequent experiments, future efforts should focus on two key areas: promoting cation ordering to achieve a well-ordered layered structure and mitigating Ni/Li deficiencies to reduce undesirable cation mixing. Our work will concentrate on synthesizing a material with a perfect layered structure, characterized by a higher intensity ratio of the (003) to (104) XRD peaks ($I_{003}/I_{104} > 1$). Achieving this structural refinement is expected to yield higher practical specific charge/discharge capacities.

Conflict of interest: *The authors declare no conflict of interest.*

Acknowledgement: *This work was supported by the National Academy of Sciences of Ukraine under project No. 0123U101087, "Development of a method for recovery of active materials after degradation of lithium-ion batteries".*

References

[1] Y. Jin, X. Qu, L. Ju, Z. Zhou, W. Sun, L. Song, M. Zhang, Sustainable regeneration of a spent layered lithium nickel cobalt manganese oxide cathode from a scrapped lithium-ion battery, *Journal of Materials Chemistry A* **12** (2024) 32613-32637. https://doi.org/10.1039/D4TA05089D

[2] J. Quan, S. Zhao, D. Song, T. Wang, W. He, G. Li, Comparative life cycle assessment of LFP and NCM batteries including the secondary use and different recycling technologies, *Science of the Total Environment* **819** (2022) 153105. https://doi.org/10.1016/j.scitotenv.2022.153105
[3] S. Natarajan, V. Aravindan, Recycling strategies for spent Li-ion battery mixed cathodes, *ACS Energy Letters* **3** (2018) 2101-2103. https://doi.org/10.1021/acsenergylett.8b01233
[4] M. Buchert, W. Jenseit, C. Merz, D. Schüler, *Verbundprojekt: Entwicklung eines realisierbaren Recyclingkonzepts für die Hochleistungsbatterien zukünftiger Elektrofahrzeuge - LiBRi: Teilprojekt: LCA der Recyclingverfahren*, Oeko-Institut, Darmstadt, Germany, 2011. https://www.oeko.de/oekodoc/1499/2011-068-de.pdf (in German)
[5] J. Li, J. Fleetwood, W. B. Hawley, W. Kays, From materials to cell: State-of-the-art and prospective technologies for lithium-ion battery electrode processing, *Chemical Reviews* **122** (2022) 903-956. https://doi.org/10.1021/acs.chemrev.1c00565
[6] R. Tao, Y. Gu, Z. Du, X. Lyu, J. Li. Advanced electrode processing for lithium-ion battery manufacturing, *Nature Reviews Clean Technology* **1** (2025) 116-131. https://doi.org/10.1038/s44359-024-00018-w
[7] N. Hayagan, I. Gaalich, P. Loubet, L. Croguennec, C. Aymonier, G. Philippot, J. Olchowka, Challenges and perspectives for direct recycling of electrode scraps and end-of-life lithium-ion batteries, *Batteries and Supercaps* **7** (2024) e202400120. https://doi.org/10.1002/batt.202400120
[8] H. Ji, J. Wang, J. Ma, H. M. Cheng, G. Zhou, Fundamentals, status and challenges of direct recycling technologies for lithium ion batteries, *Chemical Society Reviews* **52** (2023) 8194-8244. https://doi.org/10.1039/D3CS00254C
[9] S. O. Oriekhov, O. V. Potapenko, V. A. Sirosh. Extraction of elements from the cathode mass of a lithium-nickel-cobalt-manganese oxide-based battery. *Ukrainian Conference with International Participation "Chemistry, physics and technology of surface" dedicated to the 95-th birthday of Academician Oleksii Chuiko*, Kyiv, Ukraine, 2025, p. 169. ISBN 978-617-95367-2-4
[10] B. Halyuk, A. Mishuk, R. Derkach, V. Barsukov. Recycling of spent lithium-ion battery cathodes using electrolysis. *Promising Materials and Processes in Applied Electrochemistry*, Kyiv, Ukraine, 2024, p. 47-52. ISBN 978-617-7763-42-9
[11] A. Zanoletti, A. Mannu, A. Cornelio, Solvometallurgy as alternative to pyro- and hydrometallurgy for lithium, cobalt, nickel, and manganese extraction from black mass processing: State of the art, *Materials* **18** (2025) 2761. https://doi.org/10.3390/ma18122761
[12] A. B. Shrestha, A. S. Amarasekara, The sustainable and green management of spent lithium-ion batteries through hydroxy acid Recycling and direct regeneration of active positive electrode material: A Review, *Batteries* **11** (2025) 68-90. https://doi.org/10.3390/batteries11020068
[13] O. V. Potapenko, O. I. V'yunov, H. V. Potapenko, K. I. Vavilon, O. A. Vyshnevskyi, V. A. Sirosh, V. O. Oliinyk, Efficient Hydrometallurgical Recycling of Lithium iron-phosphate batteries using the acetic acid, *Chemistry, Physics and Technology of Surface* **16** (2025) 463-473. https://doi.org/10.15407/hftp16.04.463
[14] Z. J. Baum, R. E. Bird, X. Yu, J. Ma, Lithium-Ion Battery Recycling Overview of Techniques and Trends, *ACS Energy Letters* **7** (2022) 712-719. https://doi.org/10.1021/acsenergylett.1c02602
[15] F. Larouche, F. Tedjar, K. Amouzegar, G. Houlachi, P. Bouchard et al. Progress and Status of Hydrometallurgical and Direct Recycling of Li-Ion Batteries and Beyond. *Materials* **13** (2020) 801. https://doi.org/10.3390/ma13030801
[16] Q. Guo, J. Huang, Z. Liang, H. Potapenko, M. Zhou, X. Tang, S. Zhong, The use of a single-crystal nickel-rich layered NCM cathode for excellent cycle performance of lithium-ion batteries. *New Journal of Chemistry* **45** (2021) 3652-3659. https://doi.org/10.1039/D0NJ05914E
[17] J. Wang, J. Li, S. Li, W. Du, Y. Xu, K. Wang, An oxide precursor route for manufacturing nickel-rich NCM cathode materials through the flame synthesis approach, *Progress in Natural Science: Materials International* **35** (2025) 485-491. https://doi.org/10.1016/j.pnsc.2025.04.001

(cc) BY

[18] X. Xu, H. Huo, J. Jian, L. Wang, H. Zhu, S. Xu, X. He, G. Yin, C. Du, X. Sun, Radially oriented single-crystal primary nanosheets enable ultrahigh rate and cycling properties of $LiNi_{0.8}Co_{0.1}Mn_{0.1}O_2$ cathode material for lithium-ion batteries, *Advanced Energy Materials* **9** (2019) 1803963. https://doi.org/10.1002/aenm.201803963

[19] A. K. Nikumbh, A. E. Athare, V. B. Raut, A study of the thermal decomposition of cobalt (II) and nickel (II) oxalate dihydrate using direct current electrical conductivity measurements, *Thermochimica Acta* **186** (1991) 217-233. https://doi.org/10.1016/0040-6031(91)87038-X

[20] F. Wu, J. Tian, Y. Su, J. Wang, C. Zhang, L. Bao, T. He, J. Li, S. Chen, Effect of Ni^{2+} content on lithium/nickel disorder for Ni-Rich cathode materials, *ACS Applied Materials & Interfaces* **7** (2015) 7702-7708. https://doi.org/10.1021/acsami.5b00645

[21] S. Bhanuchandar, G. Vinothkumar, P. Arunkumar, M. Sribalaji, A. K. Keshri, K. S. Babu,. Unravelling the role of cationic Ni^{2+} vacancies and Ni^{3+} ions in non-stoichiometric NiO: breakdown of anti-ferromagnetic ordering and large exchange bias, *Journal of Materials Science* **58** (2023) 13136-13153. https://doi.org/10.1007/s10853-023-08853-1

[22] Z. Fu, J. Hu, W. Hu, S. Yang, Y. Luo, Quantitative analysis of Ni^{2+}/Ni^{3+} in $Li[Ni_xMn_yCo_z]O_2$ cathode materials: Non-linear least-squares fitting of XPS spectra, *Applied Surface Science* **441** (2018) 1048-1056. https://doi.org/10.1016/j.apsusc.2018.02.114

[23] S. O. Ajayi, C. O. Ehi-Eromosele, X. Liu, M. K. Mathe, Improving cycling performance and high rate capability of $LiNi_{0.5}Mn_{0.3}Co_{0.2}O_2$ cathode materials by sol-gel combustion synthesis, *Journal of Physics and Chemistry of Solids* **196** (2025) 112352. https://doi.org/10.1016/j.jpcs.2024.112352

[24] J. Xu, J. Yang, S. Wang, J. Jiang, Q. Zhuang, X. Qiu, K. Wu, H. Zheng, Ion transport and electrochemical reaction in $LiNi_{0.5}Co_{0.2}Mn_{0.3}O_2$-based high energy/power lithium-ion batteries, *Nanomaterials* **13** (2023) 856-870. https://doi.org/10.3390/nano13050856

[25] E. D. Orlova, A. A. Savina, S. A. Abakumov, A. V. Morozov, A. M. Abakumov, Comprehensive study of Li^+/Ni^{2+} disorder in Ni-rich NMCs cathodes for Li-ion batteries, *Symmetry* **13** (2021) 1628-1642. https://doi.org/10.3390/sym13091628

[26] J. Li, G. Liang, W. Z. Zhang, S. Zhang, K. Davey, W. K. Pang, Z. Guo, Addressing cation mixing in layered structured cathodes for lithium-ion batteries: A critical review, *Nano Materials Science* **5** (2023) 404-420. https://doi.org/10.1016/j.nanoms.2022.09.001

[27] X. Li, B. Su, W. Xue, J. Zhang, Synthesis and electrochemical characterization of $LiNi_{0.5}Co_{0.2}Mn_{0.3}O_2$ cathode material by solid-phase reaction, *Materials* **15** (2022) 3931-3940. https://doi.org/10.3390/ma15113931

[28] J. Zheng, Y. Ye, T. Liu, Y. Xiao, C. Wang, F. Wang, F. Pan. Ni/Li disordering in layered transition metal oxide: Electrochemical impact, origin, and control, *Accounts of Chemical Research* **52** (2019) 2201-2209. https://doi.org/10.1021/acs.accounts.9b00033

©2026 by the authors; licensee IAPC, Zagreb, Croatia. This article is an open-access article distributed under the terms and conditions of the Creative Commons Attribution license (http://creativecommons.org/licenses/by/4.0/)